



Deposited via The University of Leeds.

White Rose Research Online URL for this paper:

<https://eprints.whiterose.ac.uk/id/eprint/115279/>

Version: Accepted Version

---

**Article:**

Riddick, SN, Blackall, TD, Dragosits, U et al. (2017) High temporal resolution modelling of environmentally-dependent seabird ammonia emissions: Description and testing of the GUANO model. *Atmospheric Environment*, 161. pp. 48-60. ISSN: 1352-2310

<https://doi.org/10.1016/j.atmosenv.2017.04.020>

---

© 2017, Elsevier. Licensed under the Creative Commons Attribution-NonCommercial-NoDerivatives 4.0 International <http://creativecommons.org/licenses/by-nc-nd/4.0/>

**Reuse**

Items deposited in White Rose Research Online are protected by copyright, with all rights reserved unless indicated otherwise. They may be downloaded and/or printed for private study, or other acts as permitted by national copyright laws. The publisher or other rights holders may allow further reproduction and re-use of the full text version. This is indicated by the licence information on the White Rose Research Online record for the item.

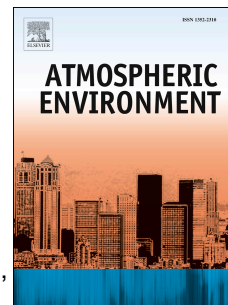
**Takedown**

If you consider content in White Rose Research Online to be in breach of UK law, please notify us by emailing [eprints@whiterose.ac.uk](mailto:eprints@whiterose.ac.uk) including the URL of the record and the reason for the withdrawal request.

# Accepted Manuscript

High temporal resolution modelling of environmentally-dependent seabird ammonia emissions: Description and testing of the GUANO model

S.N. Riddick, T.D. Blackall, U. Dragosits, Y.S. Tang, A. Moring, F. Daunt, S. Wanless, K.C. Hamer, M.A. Sutton



PII: S1352-2310(17)30258-3

DOI: [10.1016/j.atmosenv.2017.04.020](https://doi.org/10.1016/j.atmosenv.2017.04.020)

Reference: AEA 15287

To appear in: *Atmospheric Environment*

Received Date: 5 December 2016

Revised Date: 29 March 2017

Accepted Date: 12 April 2017

Please cite this article as: Riddick, S.N., Blackall, T.D., Dragosits, U., Tang, Y.S., Moring, A., Daunt, F., Wanless, S., Hamer, K.C., Sutton, M.A., High temporal resolution modelling of environmentally-dependent seabird ammonia emissions: Description and testing of the GUANO model, *Atmospheric Environment* (2017), doi: 10.1016/j.atmosenv.2017.04.020.

This is a PDF file of an unedited manuscript that has been accepted for publication. As a service to our customers we are providing this early version of the manuscript. The manuscript will undergo copyediting, typesetting, and review of the resulting proof before it is published in its final form. Please note that during the production process errors may be discovered which could affect the content, and all legal disclaimers that apply to the journal pertain.

# 1 High temporal resolution modelling of environmentally-dependent 2 seabird ammonia emissions: description and testing of the GUANO 3 Model

4 S. N. Riddick<sup>1,2,3</sup>, T. D. Blackall<sup>2</sup>, U. Dragosits<sup>1</sup>, Y.S. Tang<sup>1</sup>, A. Moring<sup>1,5</sup>, F. Daunt<sup>1</sup>,  
5 S. Wanless<sup>1</sup>, K. C. Hamer<sup>4</sup> and M. A. Sutton<sup>1</sup>

6 <sup>1</sup> Centre for Ecology & Hydrology Edinburgh, Bush Estate, Penicuik, Midlothian,  
7 EH26 0QB, UK

8 <sup>2</sup> Department of Geography, King's College London, Strand, London, WC2R 2LS,  
9 UK

10 <sup>3</sup> now at Department of Civil and Environmental Engineering, Princeton University,  
11 Princeton, 08540, USA

12 <sup>4</sup> School of Biology, University of Leeds, Leeds, LS2 9JT, UK

13 <sup>5</sup> School of Geosciences, University of Edinburgh, EH9 3FE, UK

## 14 Abstract

15 Many studies in recent years have highlighted the ecological implications of adding  
16 reactive nitrogen ( $N_r$ ) to terrestrial ecosystems. Seabird colonies represent a situation  
17 with concentrated sources of  $N_r$ , through excreted and accumulated guano, often  
18 occurring in otherwise nutrient-poor areas. To date, there has been little attention  
19 given to modelling N flows in this context, and particularly to quantifying the  
20 relationship between ammonia ( $NH_3$ ) emissions and meteorology. This paper presents  
21 a dynamic mass-flow model (GUANO) that simulates temporal variations in  $NH_3$   
22 emissions from seabird guano. While the focus is on  $NH_3$  emissions, the model  
23 necessarily also treats the interaction with wash-off as far as this affects  $NH_3$ . The  
24 model is validated using  $NH_3$  emissions measurements from seabird colonies across a  
25 range of climates, from sub-polar to tropical. In simulations for hourly time-resolved  
26 data, the model is able to capture the observed dependence of  $NH_3$  emission on  
27 environmental variables. With temperature and wind speed having the greatest effects  
28 on emission for the cases considered. In comparison with empirical data, the  
29 percentage of excreted nitrogen that volatilizes as  $NH_3$  is found to range from 2% to  
30 67% (based on measurements), with the GUANO model providing a range of 2% to  
31 82%. The model provides a tool that can be used to investigate the meteorological  
32 dependence of  $NH_3$  emissions from seabird guano and provides a starting point to  
33 refine models of  $NH_3$  emissions from other sources.

## 34 1. Introduction

35 Reactive nitrogen ( $N_r$ ) has been used to improve crop growth for the last 8,000 years  
36 (Bogaard et al., 2013). However,  $N_r$  used as either manure or synthetic fertilizer has  
37 increased globally from approximately 21 Tg N yr<sup>-1</sup> in 1850 to 185 Tg N yr<sup>-1</sup> in 2000  
38 (Potter et al., 2010). The consequences of applying  $N_r$  to a surface depend on the  
39 climatic conditions, the properties of the substrate and the surrounding vegetation.  
40 Reactive nitrogen can either run off during rain events, become part of the  
41 surrounding ecosystem (immobilized in the soil or absorbed by plants) or volatilize as  
42 nitrogen-based gas: ammonia ( $NH_3$ ), nitrous oxide ( $N_2O$ ), nitrogen oxides ( $NO_x$ ) or  
43 nitrogen ( $N_2$ ). The rate of formation and volatilization of  $NH_3$  from  $N_r$  is highly  
44 temperature dependent (Sutton et al., 2013; Riddick et al., 2012; 2014) and  $NH_3$

45 emission has been linked with acidification and eutrophication close to the emissions  
46 site (Sutton et al., 2012) and changes in radiative forcing globally (Adams et al.,  
47 2001).

48 The largest seabird colonies are found in remote areas far from human interaction  
49 (Riddick et al., 2012). At such locations seabird nitrogen excreta is the dominant  
50 source of  $N_r$  making seabird colonies ideal “natural laboratories” to investigate  
51 biogeochemical processes and the resulting impact of  $N_r$  pathways on plants and  
52 animals. Studies have shown that seabirds are significant sources of  $NH_3$  (Wilson et  
53 al. 2004, Blackall et al. 2007, Zhu et al., 2011; Riddick et al., 2014; 2016) and have a  
54 large spatial impact in both the Arctic (Wentworth et al., 2015) and Antarctic  
55 (Theobald et al. 2013, Crittenden et al., 2015. Changes in atmospheric composition  
56 across the entire Baffin Bay region were attributed to seabird  $NH_3$  (Wentworth et al.,  
57 2015), while a study of Adelie penguin colony on the Antarctic continent suggested  
58 that volatilized  $NH_3$  creates a spatial impact zone of up to 300 km<sup>2</sup> surrounding the  
59 colony where phosphomonoesterase activity is increased in lichen populations  
60 (Crittenden et al., 2015).

61 Given the local and global importance of  $NH_3$  emissions, two main methods have  
62 been used to estimate  $NH_3$  emissions from  $N_r$  sources, which are broadly described as  
63 empirically derived emission factors and process-based models. The former use  
64 empirical data to integrate the effects of meteorology into a single value (‘emission  
65 factor’) that can be used, for example, to estimate emission of a particular animal  
66 species. Alternatively, the emission can be estimated based on a percentage of  $N_r$  that  
67 volatilizes as  $NH_3$ , e.g. on average 21 % of N in manure volatilizes as  $NH_3$  in  
68 industrialized countries (Bouwman et al., 2002).

69 Process-based models attempt to replicate the effects of meteorology on the formation  
70 of  $NH_3$  from an  $N_r$  source.  $NH_3$  volatilization has been shown to increase at both high  
71 temperatures and high wind speeds (Demmers et al., 1998; Sommer & Christensen,  
72 1991), while rain events may cause  $NH_3$  emissions to drop to almost zero, as  
73 illustrated by Sommer & Olesen (2000) for liquid manure spreading in Denmark.  
74 Most recent models calculate  $NH_3$  fluxes using Henry’s Law, i.e. the dissociation  
75 reactions of ammonium and  $NH_3$  in solution is used to calculate the  $NH_3$  gas on the  
76 surface, with the flux estimated using a resistance-based approach (e.g. Sutton et al.,  
77 1998; Cooter et al., 2010; Massad et al., 2010; Flechard et al., 2013). For instance,  
78 Cooter et al. (2010) used a process-based model to predict measured diurnal variation  
79 and daily means of  $NH_3$  emissions from agricultural soils.

80 Even though Henry’s Law has been used to calculate  $NH_3$  emissions from  $N_r$  sources,  
81 these models have not been explicitly validated with high resolution empirical  
82 measurements from a range of meteorological conditions. For example, Massad et al.  
83 (2010) reviewed existing measurements to compile a comprehensive dataset and  
84 derived generalized parameterizations for a range of fertilizers and ecosystems to be  
85 used in large-scale chemical transport and earth system models. Flechard et al. (2013)  
86 synthesized data from a range of studies to generate consistent parameterizations that  
87 can be used to calculate  $NH_3$  emissions on the regional and global scale. Cooter et al.  
88 (2010) used their model to calculate  $NH_3$  emissions at the field scale and compared  
89 their model output to fertilizer application at a site in North Carolina, USA.

90 In an initial approach to modelling  $NH_3$  emissions from seabirds, only the  
91 bioenergetics part of the GUANO model was used, linked to empirical estimates of

92 the percentage volatilized (Wilson et al. 2004, Blackall et al., 2007). This approach  
93 provided an adequate description of the spatial differences in NH<sub>3</sub> emissions on a  
94 regional and country scale. However, it meant that there was a high uncertainty in the  
95 estimates in the extrapolations to a global scale by Blackall et al. (2007).

96 A first approach to address this uncertainty was provided by Riddick et al. (2012) who  
97 used an empirical temperature correction, with uncertainty ranges of estimates based  
98 on a) no temperature dependence and b) full solubility dependence according to the  
99 thermodynamics of Henry's Law and ammonium dissociation. If, like Blackall et al.  
100 (2007), they ignored the possible effect of temperature, then they found total global  
101 NH<sub>3</sub> emissions from seabirds of 442 Gg NH<sub>3</sub> year<sup>-1</sup> (where penguins contributed 83%,  
102 due to improved bird statistics). By contrast, if NH<sub>3</sub> emissions were proportional to  
103 the thermodynamic effect of temperature, they found total global NH<sub>3</sub> emission from  
104 seabirds to be only 97 Gg NH<sub>3</sub> year<sup>-1</sup> (where penguins contributed 63%). According  
105 to a mid-range estimate of the temperature dependence, they estimated 270 Gg NH<sub>3</sub>  
106 year<sup>-1</sup> (with 80% from penguins). Penguins were thus estimated to be the main source  
107 of NH<sub>3</sub> emissions from seabird colonies globally under all three scenarios, while this  
108 clearly shows the importance of addressing the temperature dependence of emissions.

109 The main limitation of Riddick et al. (2012) was the wide uncertainty range of their  
110 estimates and the need to constrain these by measurements, ideally using a process-  
111 based approach. A first application of the GUANO model reported by Sutton et al.  
112 (2013) to different sites globally showed that the main measured differences in the  
113 percentage of excreted guano that volatilizes as NH<sub>3</sub> in relation to temperature could  
114 be reproduced.

115 This paper describes the GUANO model (Generation of emissions from Uric Acid  
116 Nitrogen Outputs), a dynamic mass-flow process-based model developed to simulate  
117 NH<sub>3</sub> losses from seabird colonies. The model incorporates the main environmental  
118 factors affecting the volatilization process, allowing calculation of NH<sub>3</sub> emissions  
119 from seabird-derived N<sub>r</sub> on an hourly basis and upscaling to consider the effects of  
120 different meteorological conditions. The NH<sub>3</sub> emissions simulated by the model are  
121 compared with NH<sub>3</sub> emission estimates based on concentration measurements and  
122 turbulent exchange parameters from a climatically diverse set of seabird colonies. We  
123 use this comparison to investigate how NH<sub>3</sub> emissions from seabirds vary with  
124 changing environmental conditions.

## 125 **2. Methods and Materials**

### 126 **2.1 Outline of the GUANO model**

127 The GUANO model is designed to predict temporal variations in the formation of  
128 NH<sub>3</sub> from a source of seabird-derived uric acid (Figure 1). The model calculates NH<sub>3</sub>  
129 emissions from a seabird colony using environmental variables and colony-specific  
130 data as input. Temperature, relative humidity, precipitation and wind speed are  
131 considered to have the greatest effect on NH<sub>3</sub> formation and emission (Groot  
132 Koerkamp, 1994; Cooter et al., 2010; Massad et al., 2010; Flechard et al., 2013). The  
133 main elements of the model are described here, with additional details given in  
134 Supplementary Material Section 1.

135 <<Insert Figure 1 Here>>

136 The pathways taken by nitrogen following excretion as uric acid can be summarised  
 137 in four steps (Figure 1). Excreted guano forms uric acid (UA) that decomposes to  
 138 form total ammoniacal nitrogen (TAN), which then partitions to form gaseous  $\text{NH}_3$ .  
 139 Other pathways include wash-off of guano, UA and TAN from the surface at any  
 140 stage during rain events. It should be noted that the loss of nitrogen due to plant  
 141 uptake and immobilization, and other gaseous emissions, have not been included in  
 142 the model since these are considered to take place on a slower time scale than  $\text{NH}_3$   
 143 emissions. The following steps are included in the model:

- 144 1. Nitrogen-rich guano, in the form of UA, is excreted onto the surface by seabirds at  
 145 the colony. The amount of guano varies depending on the mass and behaviour of  
 146 the nesting species (e.g. Wilson et al. 2004). At each time-step ( $t_N$ ), the UA budget  
 147 ( $Q_{UA}$ ,  $\text{g m}^{-2}$ ) is calculated from the total nitrogen excreted ( $F_e$ ,  $\text{g m}^{-2} \text{hour}^{-1}$ ), the  
 148 TAN produced per hour ( $F_{TAN}$ ,  $\text{g m}^{-2} \text{hour}^{-1}$ ) and the Uric acid nitrogen washed off  
 149 by the rain ( $F_{w(UA)}$ ,  $\text{g m}^{-2} \text{hour}^{-1}$ ), where  $N$  is the hour of the year (Equation 1).

$$150 \quad Q_{UA}(t_{N+1}) = Q_{UA}(t_N) + F_e - F_{TAN} - F_{w(UA)} \quad (1)$$

- 152 2. Uric acid is converted to TAN, with the conversion rate depending on climatic  
 153 conditions and the pH of the surface (Elliot and Collins, 1982, Elzing and  
 154 Monteny, 1997; Groot Koerkamp et al., 1998). At each time step the TAN budget  
 155 ( $Q_{TAN}$ ,  $\text{g m}^{-2}$ ) is calculated from the TAN produced per hour from UA ( $F_{TAN}$ ,  $\text{g m}^{-2}$   
 156  $\text{hour}^{-1}$ ), the amount of  $\text{NH}_3$  emitted ( $F_{NH3}$ ,  $\text{g m}^{-2} \text{hour}^{-1}$ ) and the TAN washed off  
 157 by the rain ( $F_{w(TAN)}$ ,  $\text{g m}^{-2} \text{hour}^{-1}$ ), where  $N$  is the hour of the year (Equation 2).

$$158 \quad Q_{TAN}(t_{N+1}) = Q_{TAN}(t_N) + F_{TAN} - F_{NH3} - F_{w(TAN)} \quad (2)$$

- 160 3. TAN partitions between  $\text{NH}_4^+$  and  $\text{NH}_3$  on the surface, with the position of the  
 161 equilibrium depending on the pH and the temperature ( $T$ , K) of the surface  
 162 (Equation 3). A function,  $\Gamma = [\text{NH}_4^+]/[\text{H}^+]$ , is used to describe the equilibrium at  
 163 the surface (Nemitz et al., 2000) such that the gaseous concentration of  $\text{NH}_3$  at the  
 164 surface ( $X_c$ ) is:

$$165 \quad X_c = \frac{161500}{T} \exp\left(\frac{-10378}{T}\right) \Gamma \quad (3)$$

166 The TAN concentration is a function of the water content of the guano. The water  
 167 budget ( $Q_{H_2O}$ ,  $\text{kg m}^{-2}$ ) is calculated (Equation 4) from the flux of water contained  
 168 in excreted guano ( $F_{H_2O}(g)$ ,  $\text{kg m}^{-2} \text{hr}^{-1}$ ), rain events ( $F_{H_2O}(pptn)$ ,  $\text{kg m}^{-2} \text{hr}^{-1}$ ),  
 169 water run-off ( $F_{H_2O}(ro)$ ,  $\text{kg m}^{-2} \text{hr}^{-1}$ ) and evaporation ( $F_{H_2O}(evap)$ ,  $\text{kg m}^{-2} \text{hr}^{-1}$ ).  
 170 Each of the parameters in Equation 4 is further described in the Supplementary  
 171 Material Section 1.

$$172 \quad Q_{H_2O}(t_{N+1}) = Q_{H_2O}(t_N) + F_{H_2O}(g) + F_{H_2O}(pptn) - F_{H_2O}(ro) - F_{H_2O}(evap) \quad (4)$$

- 173 4.  $\text{NH}_3$  on the surface volatilizes to the atmosphere, with the rate of volatilization  
 174 (Equation 5) depending on the  $\text{NH}_3$  concentration difference between the surface  
 175 ( $X_c$ ) and the atmosphere ( $X_a$ ), the aerodynamic and boundary layer resistances ( $R_a$   
 176 and  $R_b$ ) (Sutton et al., 1993; Nemitz et al., 2001) estimating the effect of  $\text{NH}_3$

183 reabsorption by the substrate and any overlying vegetation using an empirical  
 184 habitat factor ( $F_{hab}$ ). A habitat factor was used here in preference to a more  
 185 process based description involving the bi-directional exchange of  $\text{NH}_3$  from  
 186 vegetation because of the complexity of the mix of nesting types. The values of the  
 187 habitat factors used are described in Section 2.2.3.

188

$$189 \quad \text{NH}_3 \text{ emission} = \frac{X_c - X_a}{R_a + R_b} F_{hab} \quad (5)$$

190

## 191 **2.2 Model input data**

192 Site-specific  $\text{NH}_3$  emissions were calculated for five seabird colonies in a range  
 193 climate zones: Tropical: Michaelmas Cay on the Great Barrier Reef (16.60 °S, 145.97  
 194 °E) and Ascension Island in the South Atlantic (7.99 °S, 14.39 °W), Temperate: the  
 195 Isle of May in Scotland (56.19 °N, 2.56 °W) and Sub-Polar: Signy Island in the South  
 196 Orkney Islands (60.72 °S, 45.60 °W) and Bird Island in South Georgia (54.0° S,  
 197 38.05° W).

### 198 **2.2.1 Meteorological input data**

199 To run the GUANO model, meteorological data are required for periods before,  
 200 during and after the measurement campaigns. Continuous monitoring of the weather  
 201 was conducted *in-situ* only on the Isle of May. For the other colonies, meteorological  
 202 data (wind speed, ground temperature, relative humidity and rainfall) were collected  
 203 during short term campaigns, with data beyond these periods obtained from the  
 204 nearest meteorological station (Table 1).

205 <<Insert Table 1 Here>>

### 206 **2.2.2 Seabird colony data**

207 The site-specific seabird data that have the greatest effect on the  $\text{NH}_3$  emission, as  
 208 identified by Wilson et al. (2004), were collated from field observations and the  
 209 literature: nest density and duration of the breeding season, adult mass, proportion of  
 210 time spent at the colony (see Table 1 also Riddick et al., 2012). The estimated total  
 211 nitrogen excreted at a colony is based on the assumption that adult seabirds excrete N  
 212 at a constant rate while at the colony and away from it.

### 213 **2.2.3 Habitat Factors**

214 Habitat factors ( $F_{hab}$ ) are used in Equation 5 to account for  $\text{NH}_3$  immobilized by the  
 215 nesting substrate or recaptured by the overlying canopy and are listed in Table 1.1 in  
 216 the Supplementary Material Section 1. This reflects a base value for bare rock of 1,  
 217 where no  $\text{NH}_3$  is immobilized or recaptured, which is then reduced as a correction  
 218 factor, to parameterise the effect of nesting behaviour of the birds. Following Wilson  
 219 et al. (2004) and the measurements of Riddick (2012), habitat factors for birds that  
 220 build nests on bare rock is taken as 1, while for those that nest on sand is taken as  
 221 0.67. For those bird species that nest on vegetation or use a nest,  $F_{hab}$  is 0.20 and  
 222 birds excreting in burrows have a  $F_{hab}$  value of 0.

223 Penguins on Bird Island and Signy Island nest on bare rock ( $F_{hab} = 1$ ), while the birds  
 224 on Michaelmas Cay and Ascension Island nest on sand ( $F_{hab} = 0.67$ ). On the Isle of  
 225 May, adult puffins make burrows, but excrete outside, while their young excrete in  
 226 burrows. Where adult puffins excrete depends on the time of day and climatic

227 conditions: at dawn and dusk, large numbers of puffins can be seen on exposed rocks  
228 across the colony, and this also happens when it is warm and sunny. For the  
229 remainder of the time, puffins excrete on the soil outside their burrow. To  
230 accommodate variations in this assumption, the  $F_{hab}$  value for adult puffins was  
231 changed from vegetation only (0.2 as estimated by Wilson et al. 2004) to an  $F_{hab}$   
232 value between rock and vegetation of 0.60 (average of 1 and 0.20). For puffin chicks,  
233 data suggest that these only excrete inside the burrows and leave the colony as soon as  
234 they leave the nest (Harris & Wanless, 2011). Puffin chicks are therefore not thought  
235 to contribute to seabird  $\text{NH}_3$  emission at the colony, with any emissions inside the  
236 burrows being absorbed by the soil inside the burrow, therefore  $F_{hab}$  for chicks is here  
237 set at 0.

#### 238 2.2.4 Other model inputs and implementation.

239 Constant values are used in the model to describe the surface roughness length ( $z_0$ )  
240 and the boundary layer Stanton number ( $B$ ) to calculate the turbulent atmospheric  
241 resistance ( $R_a$ ) and the quasi-laminar boundary layer resistance ( $R_b$ ) (Supplementary  
242 Material Section 1, equations SM21 and SM25). Constant values of 0.1 m and 5 were  
243 used in the model, and also varied as part of the model sensitivity analysis (Section  
244 2.5). Based on reference Elliot & Collins (1982), the base-rate (at pH 9 and 35°C)  
245 for the fraction of UA converted to TAN was 0.83 % day<sup>-1</sup> (Supplementary Material  
246 Section 1). The pH of the guano within the model was set at 8.5, this value was based  
247 on measurements of Blackall (2004). Factors for wash-off under rain were assumed  
248 to be 1 and 0.5 % mm<sup>-1</sup> rain for nitrogen and non-nitrogen, respectively (See  
249 Supplementary Material Section 1). Finally, based on data for remote marine  
250 environments (e.g., Sutton et al., 2003), background  $\text{NH}_3$  concentration was assumed  
251 to be 0.1  $\mu\text{g m}^{-3}$ .

252 The GUANO model was coded in Microsoft Excel. For each seabird colony the  
253 GUANO model uses meteorological and bird data to calculate the hourly  $\text{NH}_3$   
254 emission ( $\text{g NH}_3 \text{ m}^{-2} \text{ h}^{-1}$ ). The annual  $\text{NH}_3$  emission is calculated as the sum of hourly  
255 emissions. The model runs were initialized with zero UA, TAN and water in the  
256 budgets starting at least 24 months before the assessment period for comparison with  
257 the emission estimates based on concentration measurements and turbulent exchange  
258 parameters.

259

#### 260 2.3 Model validation

261 The model setup and parametrization was set based on theoretical considerations and  
262 on available data to parametrize the model. In principle, the model set up was  
263 independent of measured validation data, according to the parameters considered. In  
264 the case of substrate pH and roughness length runs were based on a constant value,  
265 while TAN and Guano run off were based on a fixed percentage per mm of rain. The  
266 habitat factors were based on prior studies drawing on Blackall (2004), Wilson et al.  
267 (2004) and Blackall et al. (2007). The only parameter which was tuned according to  
268 measurements was  $F_{hab}$  at the Atlantic Puffin site on the Isle of May, Scotland. By  
269 contrast, the model tests in comparison with measurements at Mars Bay, Ascension  
270 Island, at Bird Island, South Atlantic, at Michaelmas Cay, Great Barrier Reef, at  
271 Signy Island, South Atlantic were made without tuning any other model parameters

272 and therefore represent fully independent tests of the model in a wide range of  
273 climatic conditions.

### 274 **2.3.1 Measured NH<sub>3</sub> emissions for comparison with the model**

275 Two methods were employed to conduct NH<sub>3</sub> concentration emission estimates based  
276 on concentration measurements and turbulent exchange parameters, which were used  
277 to quantify NH<sub>3</sub> emissions, as reported in detail by Riddick et al. (2014): (1) passive  
278 sampling and (2) active on-line NH<sub>3</sub> analysis instrument. For the passive sampler  
279 measurements (ALPHA samplers, CEH Edinburgh, Tang et al., 2001), triplicate  
280 samplers were used at each sampling location and exposed for periods of 2 to 4 weeks  
281 to measure an average concentration for the exposure period. The time-averaged NH<sub>3</sub>  
282 concentration data were then used with the WindTrax inverse dispersion model  
283 version 2.0 to calculate the emission (Flesch et al., 1995; Riddick et al. 2014).

284 Active on-line NH<sub>3</sub> concentration measurements were made by Riddick et al. (2014,  
285 2016) with an AiRRmonia gas analyser (Mechatronics, NL) on Bird Island and  
286 Ascension Island and a Nitrolux 1000 gas analyser (Pranalytica, USA) on the Isle of  
287 May. The NH<sub>3</sub> concentration data were averaged to 15-minute data and used as input  
288 to the WindTrax in an inverse model to calculate the emission. The calculation of the  
289 NH<sub>3</sub> emissions used as validation at each of the sites are the result of five separate  
290 field campaigns and are described in full in Riddick et al. (2014) for Michaelmas Cay  
291 and Ascension Island and Riddick et al. (2016) for Signy Island, the Isle of May and  
292 Bird Island (locations of the five fieldwork sites are presented in Supplementary  
293 Material Section 2).

294 As a result of the method employed at Michaelmas Cay and Signy Island (passive  
295 sampling only), hourly resolved measured NH<sub>3</sub> fluxes were not available at these sites  
296 (Riddick et al., 2014; 2016). However, at Ascension Island (Riddick et al. 2014) and  
297 the Isle of May (Riddick et al., 2016), both passive (time integrated) measurements  
298 and the continuous measurements, were made allowing comparison between the two  
299 approaches. In both cases, close agreement was found between the passive (time-  
300 integrated) and active (time resolved) sampling methods, the uncertainty in chemical  
301 sampling method was  $\pm 20\%$  and  $\pm 12\%$  of the mean flux at the Isle of May and  
302 Ascension, respectively (Riddick et al. (2016). Calculation of a third estimate in each  
303 case (time-integrated based on the semi-continuous active sampling data) allowed it to  
304 be shown that the meteorological uncertainties associated with long measurement  
305 periods (for the passive, time-integrated measurements) were of similar magnitude to  
306 the uncertainties between the two different chemical sampling methods.

### 307 **2.3.2 Comparison modelled emissions to those estimated through measurement**

308 The GUANO model simulations were validated with emission estimates based on  
309 concentration measurements and turbulent exchange parameters from the five field  
310 sites. To assess the fit of the model, the hourly measured emissions were plotted  
311 against the hourly modelled NH<sub>3</sub> emissions, with the slope, intercept and  
312 determination coefficient ( $R^2$ ) of the linear regression calculated. Time-averaged  
313 modelled emissions are also presented and compared against matched time-averaged  
314 emission estimates based on concentration measurements and turbulent exchange  
315 parameters to show that the model, not only captures the hourly emissions, but also is  
316 consistent with measurements over a period of time.

317 In addition, the mean  $\text{NH}_3$  emission for each colony was calculated (in  $\mu\text{g m}^{-2} \text{s}^{-1}$ )  
318 from the hourly emissions. The percentage of nitrogen volatilized ( $P_v$ ) was calculated  
319 from the total nitrogen excreted at each colony during the measurement period and the  
320 total nitrogen estimated to be volatilized as  $\text{NH}_3$  over the same period.

## 321 2.4 $\text{NH}_3$ emission and meteorology

322 To investigate the effects of meteorology, the slope, intercept and  $R^2$  between  
323 modelled  $\text{NH}_3$  emission and each variable was calculated. The coefficient of  
324 determination is used to assess the size of the effect each environmental variable  
325 (ground temperature, wind speed, relative humidity and precipitation) has on the  
326 modelled  $\text{NH}_3$  emission so that the key drivers of emission at each measurement site  
327 can be identified.

## 328 2.5 Sensitivity Analysis

329 A sensitivity study was performed on the GUANO model to determine the most  
330 significant model parameters in relation to the model output. The following model  
331 parameters were investigated with realistic variations in each input parameter:  $z_0$  (m),  
332 fraction of UA converted to TAN per day, percentage nitrogen wash off ( $\% \text{ mm}^{-1}$   
333 rain), percentage non-nitrogen wash-off ( $\% \text{ mm}^{-1}$  rain), pH, habitat factors ( $F_{hab}$ ),  
334 boundary layer Stanton number ( $B$ ), temperature ( $T$ ,  $^{\circ}\text{C}$ ), relative humidity ( $RH$ ,  $\%$ ),  
335 wind speed ( $U$ ,  $\text{m s}^{-1}$ ), precipitation ( $P$ ,  $\text{mm m}^{-2} \text{hr}^{-1}$ ), net solar radiation ( $Rn$ ,  $\text{W m}^{-2}$ ),  
336 pH and background  $\text{NH}_3$  concentration ( $\mu\text{g m}^{-3}$ ). The sensitivity of the  $\text{NH}_3$  emissions  
337 to each input parameter was tested using the GUANO model application to the  
338 Atlantic puffin colony on the Isle of May. The application of the GUANO model at  
339 Isle of May was used in the sensitivity analysis because this temperate site could best  
340 respond to positive and negative changes in environmental conditions in a global  
341 context.

342

## 343 3. Results

### 344 3.1 Model output and validation with empirical data

#### 345 3.1.1 Mars Bay, Ascension Island: Sooty Tern Colony

346 The  $\text{NH}_3$  emissions calculated by the GUANO model for Ascension Island show a  
347 strong diurnal pattern, with the peak emissions corresponding to the hottest, most  
348 turbulent and windiest part of the day. The maximum measured emission during the  
349 study period was  $370 \mu\text{g NH}_3 \text{ m}^{-2} \text{ s}^{-1}$  (Figure 2). The  $\text{NH}_3$  emissions calculated by  
350 the GUANO model for Ascension Island are in close agreement to those derived from  
351 field measurements (Table 3; Supplementary Material Section 2 Figure SM 2.1), with  
352 a linear regression slope of 1.07, intercept of  $-1.20 \mu\text{g m}^{-2} \text{ s}^{-1}$  and  $R^2 = 0.94$ . The  
353 average modelled  $\text{NH}_3$  emission for Ascension Island during the measurement period  
354 was  $22.3 \mu\text{g NH}_3 \text{ m}^{-2} \text{ s}^{-1}$ , the average measured  $\text{NH}_3$  emission on Ascension was  $22.3$   
355  $\mu\text{g NH}_3 \text{ m}^{-2} \text{ s}^{-1}$  and the average modelled  $\text{NH}_3$  emission for periods when  
356 measurement data available was  $19.8 \mu\text{g NH}_3 \text{ m}^{-2} \text{ s}^{-1}$ . The most notable features of  
357 the modelled and measured  $\text{NH}_3$  emission is the strong dependence on temperature  
358 and moisture availability (with higher emissions after rain events on 25 May and 6-7  
359 June), with the TAN budget almost fully depleted before then end of each day. This  
360 implies that the  $\text{NH}_3$  emission rate is tightly coupled to the TAN production rate at  
361 this site (Supplementary Material Section 3 Figure SM 3.1; Supplementary Material

362 Section 4 Figure SM 4.1,  $R^2$  value = 0.98). At this site, aerodynamic and boundary  
363 layer resistance has little effect, as the TAN produced is all quickly lost through  $\text{NH}_3$   
364 emissions. Ammonia emission is thus hydrolysis-limited for the test period at this site,  
365 with the performance of the GUANO model therefore depending almost entirely on  
366 its parametrization the urea hydrolysis rate.

367 <<Insert Figure 2 Here>>

### 368 3.1.2 Isle of May, Scotland: Atlantic puffin Colony

369 The modelled emissions were lower for the Isle of May puffin colony than Ascension  
370 Island (Sooty tern), but showed a similar diurnal pattern (Figure 3), with high  
371 emissions in the day (maximum of  $25 \mu\text{g m}^{-2} \text{s}^{-1}$  during the afternoon) and negligible  
372 emissions at night. When compared with the emission estimates based on  
373 concentration measurements and turbulent exchange parameters, the hourly  $\text{NH}_3$   
374 emissions modelled by the GUANO model were underestimated, with a linear  
375 regression slope of 0.13, intercept of  $5.7 \mu\text{g m}^{-2} \text{s}^{-1}$  and  $R^2$  of 0.13 (Table 3;  
376 Supplementary Material Section 2 Figure SM 2.2). The poorest fit occurred on 1<sup>th</sup>  
377 July 2009, where the model overestimated the measured  $\text{NH}_3$  emission during the  
378 early hours of the morning. This was associated with a period of low-wind speed and  
379 stable conditions, which could also reflect uncertainties in the measurement estimate  
380 at this time. During the period of 29 June to 2 July the measured emissions were  
381 much smaller than model and this may correspond to a period of foggy weather where  
382  $\text{NH}_3$  could have dissolved in the fog and few puffins were seen around the colony,  
383 which may explain why the measured emissions were much smaller than the modelled  
384 emissions, which did not take account of this meteorological interaction with the  
385 ammonia gas, local bird behaviour and movements.

386 The average modelled  $\text{NH}_3$  emission for the Isle of May during the measurement  
387 period was  $7.7 \mu\text{g NH}_3 \text{ m}^{-2} \text{s}^{-1}$ , the average measured  $\text{NH}_3$  emission on the Isle of May  
388 was  $6.9 \mu\text{g NH}_3 \text{ m}^{-2} \text{s}^{-1}$  and the average modelled  $\text{NH}_3$  emission for periods when  
389 measurement data available was  $9.3 \mu\text{g NH}_3 \text{ m}^{-2} \text{s}^{-1}$ . At this site the TAN budget  
390 fluctuates greatly, with hourly modelled and measured emissions correlated with the  
391 TAN budget (Supplementary Material Section 3 Figure SM 3.2,  $R^2 = 0.05$ . In contrast  
392 to Ascension Island, however, TAN did not deplete to near zero each evening,  
393 indicating that daily  $\text{NH}_3$  emission is only partially limited by TAN production over  
394 the previous 24 hours.

395

396 <<Insert Figure 3 Here>>

### 397 3.1.3 Bird Island, South Atlantic: Macaroni Penguin Colony 'Big Mac'

398 Compared with the other seabird colonies considered in this study, a diurnal pattern  
399 was much less noticeable for both modelled and measured  $\text{NH}_3$  emissions from the  
400 Macaroni penguin colony on Bird Island (Figure 4). The maximum  $\text{NH}_3$  emission  
401 simulated by the GUANO model from the colony was  $53 \mu\text{g NH}_3 \text{ m}^{-2} \text{s}^{-1}$  at 0500 on  
402 11<sup>th</sup> December 2010. Contrary to the other sites, there was also little correlation  
403 between the emission rate and ground temperature, which was associated with small  
404 variation in ground temperature (3 - 8 °C range) during the measurement period.  
405 Instead, at this site the periods of lowest  $\text{NH}_3$  emissions (below  $10 \mu\text{g NH}_3 \text{ m}^{-2} \text{s}^{-1}$ )  
406 were observed during periods of lower wind speed, with maximum emissions during

407 periods of high wind speed, linked to a substantial range of wind speed during the  
408 measurement period (0.3 to 12 m s<sup>-1</sup>). The GUANO model simulations reproduced  
409 the measured NH<sub>3</sub> emissions well, with a linear regression slope of 1.09, and intercept  
410 of -1.32 μg m<sup>-2</sup> s<sup>-1</sup> and R<sup>2</sup> = 0.86 (Table 3; Supplementary Material Section 2 Figure  
411 SM 2.3). Modelled emissions from the Big Mac colony are mostly between 0 and 20  
412 μg m<sup>-2</sup> s<sup>-1</sup>. The average modelled NH<sub>3</sub> emission for Bird Island during the  
413 measurement period is 13.4 μg NH<sub>3</sub> m<sup>-2</sup> s<sup>-1</sup>, the average measured NH<sub>3</sub> emission on  
414 Bird Island was 12.3 μg NH<sub>3</sub> m<sup>-2</sup> s<sup>-1</sup> and the average modelled NH<sub>3</sub> emission for  
415 periods when measurement data available was 12.4 μg NH<sub>3</sub> m<sup>-2</sup> s<sup>-1</sup>.

416 At this site, the modelled TAN budget can be seen from Figure 4 to show negligible  
417 fluctuation on a daily time scale, contrary to Ascension Island and the Isle of May  
418 (Supplementary Material Section 4), while showing a slight increase over the first  
419 period and first decrease then increase over the second period. At the same time this  
420 site has much larger amounts of available TAN at the surface than these other sites, at  
421 2-3 g m<sup>-2</sup>. With relatively modest temperature fluctuations during the measurement  
422 period, at this site, the variation in NH<sub>3</sub> emission rate can therefore be seen to be  
423 primarily limited by the mass transfer process itself, as affected by wind speed and  
424 surface temperature. Supplementary Material Section 3 Figure SM 3.3 shows that  
425 there is still a significant correlation between simulated TAN production and NH<sub>3</sub>  
426 emission (R<sup>2</sup> = 0.29), the relationship is less than at the temperate and tropical sites.

427 The TAN production rate at Bird Island (0 – 0.15 g m<sup>-2</sup> hr<sup>-1</sup>) is more similar to the Isle  
428 of May (0 – 0.4 g m<sup>-2</sup> hr<sup>-1</sup>) than Ascension Island (0 – 0.1 g m<sup>-2</sup> hr<sup>-1</sup>) (Supplementary  
429 Material Section 3 Figures SM 3.1, SM 3.2 and SM 3.3). This suggests that, while  
430 temperature does not affect the daily variation, the overall magnitude of NH<sub>3</sub> emission  
431 is still largely controlled by TAN hydrolysis rate. i.e. hydrolysis rate controls the  
432 overall rate of emission while meteorology controls the short-term variation in NH<sub>3</sub>  
433 emission.

434 <<Insert Figure 4 Here>>

#### 435 3.1.4 Michaelmas Cay, Great Barrier Reef: Common noddy colony

436 The NH<sub>3</sub> emissions simulated by the GUANO model for Michaelmas Cay show a  
437 strong diurnal pattern, with maximum emissions during the day reaching nearly 500  
438 μg m<sup>-2</sup> s<sup>-1</sup> which drop to an emission during the night of between 1 and 10 μg m<sup>-2</sup> s<sup>-1</sup>.  
439 The average NH<sub>3</sub> emission measured using passive samplers for two periods of four  
440 weeks during November and December (Riddick et al., 2014) are very similar to the  
441 emissions simulated by the GUANO model when averaged over the same periods  
442 (Figure 5A and Table 2). The NH<sub>3</sub> emissions measured during the field campaign are  
443 25.9 μg NH<sub>3</sub> m<sup>-2</sup> s<sup>-1</sup>. Both measured and modelled emission showed an increase from  
444 November to December. The average NH<sub>3</sub> emission predicted by the GUANO model  
445 is 27.5 μg NH<sub>3</sub> m<sup>-2</sup> s<sup>-1</sup> for November and December 2009.

446 The modelled TAN budget showed a high level of temporal structure, combining both  
447 substantial diurnal variations (indicating some limitation according to the TAN  
448 production rate) and some variation due to mass transfer limitations under the control  
449 of temperature and other environmental variables (see Supplementary Material  
450 Section 3 Figure SM 3.4, where simulated TAN production rate and simulated NH<sub>3</sub>  
451 emission are found to be correlated with R<sup>2</sup> = 0.91).

452 <<Insert Figure 5 Here>>

453 <<Insert Table 2 Here>>

### 454 3.1.5 Signy Island, South Atlantic: Chinstrap penguin Colony

455 As with the tropical and temperate regions, but in contrast to the other sub-polar  
456 colony at Bird Island, NH<sub>3</sub> emissions simulated for Signy by the GUANO model were  
457 strongly diurnal (Figure 5B). This can be explained by the more regular diurnal  
458 variation in temperature (typically 4-6° C diurnal change) than at Bird Island (Figure  
459 4).

460 The Signy Island colony is used by both Adélie and Chinstrap penguins for the first  
461 measurement period. During the second period, the Adélie penguins gradually left the  
462 colony and only Chinstrap penguins were present for the third period. The NH<sub>3</sub>  
463 emissions at Signy Island are the highest for the first period, reaching a maximum of  
464 50.0 µg NH<sub>3</sub> m<sup>-2</sup> s<sup>-1</sup>. The average NH<sub>3</sub> emission predicted by the GUANO model for  
465 the penguin colony during the whole measurement period was 10.7 µg NH<sub>3</sub> m<sup>-2</sup> s<sup>-1</sup>.  
466 This is similar to the NH<sub>3</sub> emissions measured during the field campaign of 9.0 µg  
467 NH<sub>3</sub> m<sup>-2</sup> s<sup>-1</sup> (Table 2).

468 The simulated TAN budget for the penguin colony at Signy Island shows negligible  
469 diurnal variation, but rather a steady increase through the study period from 30 to 55 g  
470 m<sup>-2</sup> (Figure 5). Overall, there was only a weak correlation between simulated TAN  
471 production and simulated NH<sub>3</sub> emission (Supplementary Material Section 3 Figure  
472 SM 3.5). The reason for the smooth trend in TAN budget at the surface (Figure 5b) is  
473 that the NH<sub>3</sub> emissions and run off during the study period represent only small  
474 fraction of the TAN produced (Supplementary Material Section 4 Figure SM 4.5).  
475 The values of the TAN budget at Signy Island are much higher than the other sites  
476 because of the lower temperatures that allow TAN to accumulate rather than  
477 volatilize.

478

### 479 3.2 NH<sub>3</sub> Emissions and environmental conditions

480 Considering the simulated estimates from the GUANO model at each site, the  
481 strongest meteorological driver of NH<sub>3</sub> emission was found to be ground temperature  
482 for all sites except for Bird Island, average  $R^2$  of 0.29 (range 0.11 - 0.39) (Table 3).  
483 As ground temperature increases, the rate of bacterial decomposition of uric acid  
484 nitrogen to form TAN (Equation 2) increases and, coupled with an increased volatility  
485 of NH<sub>3</sub> (Equation 3), results in increased NH<sub>3</sub> emission.

486 The next strongest driver of NH<sub>3</sub> emission is wind speed, with an average  $R^2$  of 0.18  
487 (range 0.01 - 0.59), with the highest correlation on Bird Island ( $R^2 = 0.59$ ) where there  
488 was a wide range of wind speeds and small differences in temperature. Relative  
489 humidity and precipitation were not found to be strong climatic drivers of NH<sub>3</sub>  
490 emission, with  $R^2$  values ranging from 0.01 to 0.04. This is not to say that these  
491 factors are unimportant, as the response of both modelled and measured NH<sub>3</sub> emission  
492 to precipitation at Ascension Island showed (Figure 2). Precipitation and relatively  
493 humidity are fundamental controls on TAN formation from UA and influences NH<sub>3</sub>  
494 emission on a longer time scale than variation in temperature and wind speed which  
495 directly affects the hourly variation in NH<sub>3</sub> emissions.

496 The importance of moisture availability which is absorbed by guano may be more  
497 easily seen in the measured long-term response, where Michaelmas Cay had a higher

498 measured percentage volatilization ( $P_v = 67\%$ ) as compared with Ascension Island ( $P_v$   
499  $= 52\%$ ) even though the sites had similar average temperature (Tables 1 and 3). This  
500 may be reflective of more moisture limitation to uric acid hydrolysis at Ascension  
501 Island. This difference is supported by the GUANO model simulation which also  
502 estimated a higher value of  $P_v$  for Michaelmas Cay (82%) than for Ascension Island  
503 (37%), reflecting the generally higher simulated guano water content at Michaelmas  
504 Cay than at Ascension Island (Figures 5A and 2).

505 <<Insert Table 3 Here>>

### 506 3.5 Sensitivity analysis

507 A sensitivity analysis of the GUANO model is shown in Table 4 for each input  
508 variable selected. The estimated  $\text{NH}_3$  emissions were most sensitive to changes in  
509 environmental variables, with highest sensitivity to ground temperature which varied  
510 by +59.9 % to -36.8 % for changes of +10% and -10%, respectively. The  $\text{NH}_3$   
511 emissions calculated by the GUANO model had the smallest response to changes in  
512 micrometeorological constants used to calculate the flux, i.e. surface roughness,  
513 boundary layer Stanton number and background  $\text{NH}_3$  concentration.

514 Of the constants used, the GUANO model is most sensitive the substrate pH. The  
515 model uses a substrate pH equal to the pH of guano, estimated at 8.5 (hydron  
516 concentration:  $[\text{H}^+] = 3.2\text{E-}9$ ) by Blackall (2004), and changes in pH from pH 7 ( $[\text{H}^+]$   
517  $= 1\text{E-}7$ ) to pH 10 ( $[\text{H}^+] = 1\text{E-}10$ ) result in 73 % and -22 % effect on  $\text{NH}_3$  emission,  
518 respectively. The sensitivity in the model to pH is caused by the  $\Gamma$  function, which is  
519 used to describe the equilibrium of the concentrations of the TAN and hydrogen ions  
520 on the surface (Equation SM18), and is directly proportional to the gaseous  
521 concentration of  $\text{NH}_3$  at the surface (Equation 3). We recognize that this is a source  
522 of uncertainty in the model, however the value used in the GUANO model for  
523 substrate pH is currently the best available.

524 The sensitivity of the modelled emission to changing environmental conditions can be  
525 seen in Supplementary Material Section 6, where in all cases the  $\text{NH}_3$  emission  
526 increases with ground temperature and in all cases emissions is the same at 25 °C.  
527 Wind speed has the next biggest effect as  $\text{NH}_3$  emission increases with wind speed at  
528 low temperatures. Precipitation also affects emission as higher rainfall results in  
529 lower emission at low temperatures. Relative humidity has relatively little effect on  
530 emission, but higher humidity results in lower emission.

531

## 532 4 Discussion

### 533 4.1 General Discussion

534 This paper presents and describes the GUANO model, the first dynamic mass-flow  
535 process-based model developed to simulate  $\text{NH}_3$  losses from seabird guano, which is  
536 here validated against  $\text{NH}_3$  emissions measured at seabird colonies representative of a  
537 range of climates around the world. Comparison with  $\text{NH}_3$  emission estimates based  
538 on measurements of  $\text{NH}_3$  concentration and turbulent exchange parameters (Riddick  
539 et al., 2014; 2016) shows that the model is able to reproduce the magnitude and  
540 temporal variation of  $\text{NH}_3$  emissions for a broad range of nesting habitats and climatic  
541 conditions. The GUANO model has been structured to simulate hourly  $\text{NH}_3$   
542 emission, using nitrogen excretion rates, temperature, relative humidity, wind speed

543 and precipitation. This choice of time resolution, however, is purely a matter of model  
544 implementation and the model has the flexibility to allow for this to be changed.  
545 However, the advantage of calculating hourly emission estimates is that the GUANO  
546 model is able to discriminate the main effects of varying environmental conditions  
547 including diurnal variability. In this way, a clearer picture emerges of the main  
548 controls on  $\text{NH}_3$  emissions from seabird colonies.

549 The model parametrization was based primarily on well-established existing  
550 principles and measured terms. Elements such as the turbulent and laminar boundary  
551 layer resistances have been widely used in other models, where the main uncertainty  
552 concerns the setting of the surface roughness length. Here we used an estimate based  
553 on observational data (Riddick et al. 2014; 2016) and Seinfeld and Pandis (2006) to  
554 set the roughness length at 0.1 m. The emission itself is driven by the concentration  
555 difference between atmospheric  $\text{NH}_3$  concentrations and the surface  $\text{NH}_3$   
556 concentration. However, as the former is very small, the key uncertainty is the surface  
557  $\text{NH}_3$  concentration. The first challenge is to simulate the rate of uric acid hydrolysis,  
558 for which we used a parametrization unchanged from Elliot and Collins (1982), based  
559 on measurements from a poultry house context. The fact that this delivers good  
560 agreement with observed fluxes in a context where  $\text{NH}_3$  emission is limited almost  
561 entirely by UA hydrolysis rate (Ascension Island), provides strong support for the  
562 parametrization of Elliot and Collins (1982). The other major uncertainties in the  
563 model concern surface pH, the habitat factor and the extent of wash-off. For the  
564 surface pH use of a prior measurement estimate from Blackall (2004) for all  
565 modelling sites shows that a fixed value of pH 8.5 is sufficient for the model  
566 application. The  $F_{hab}$  could be considered as a model tuning parameter, however, this  
567 would only apply for sites not on bare rock (for which  $F_{hab} = 1$ ). The reduction factors  
568 used in this study were in fact based on prior estimates from Wilson et al. (2004) with  
569 the only changes for this study being at the Atlantic puffin site on the Isle of May  
570 where  $F_{hab}$  was taken as an average of rock and vegetation nesters to reflect the  
571 variability of the bird's behaviour. For the wash off factors, constant relationship for  
572 all sites was used of 1 and 0.5 %  $\text{mm}^{-1}$  rain for nitrogen and non-nitrogen,  
573 respectively. While this is an extremely simple approach, its value was based on  
574 Blackall (2004) and thus set as a prior value rather than being used to fit the  
575 measurements. Overall, therefore, it can be seen that while the performance of the  
576 model runs is sensitive to the model parametrization, the parameter choices were  
577 largely based on prior estimates independently from the outcome of the  
578 measurements.

579 The comparison of the GUANO model output with  $\text{NH}_3$  emission estimates based on  
580 concentration measurements and turbulent exchange parameters at a range of sites  
581 showed the GUANO model is able to reasonably model the  $\text{NH}_3$  emissions in  
582 different climate regions (Table 3), while giving better agreement with observations  
583 than any single environmental variable. Hourly measurements at the different field  
584 sites had  $R^2$  values between model and measurements of between 0.5 and 0.9 (Table  
585 3), while  $R^2$  values with other environmental variables were generally lower.

586 The model-measurement comparison also illustrates how the different primary  
587 controls on  $\text{NH}_3$  emissions at the different sites. Sufficient water is needed for uric  
588 acid hydrolysis (as shown at Ascension Island), while excess water dilutes the TAN  
589 solution and is associated with increased TAN run off (Bird Island). The combined

590 outcome of these effects is that increases in relative humidity or rain events only  
591 increase simulated NH<sub>3</sub> emissions at arid sites such as Ascension Island (Figure 2).

592 The NH<sub>3</sub> emissions simulated by the GUANO model increased with wind speed at all  
593 sites because vertical transport and turbulent mixing of NH<sub>3</sub> increases as aerodynamic  
594 and boundary layer resistances decrease. However, wind speed was only the major  
595 driver of NH<sub>3</sub> emission variations at a windy site with little variation in ground  
596 temperature (Bird Island). At the other sites, ground temperature was the major driver  
597 in temporal differences of NH<sub>3</sub> emission. Temperature is significant for two reasons:  
598 (1) it affects the rate at which uric acid converts to NH<sub>3</sub> and (2) it affects the potential  
599 for volatilization of NH<sub>3</sub> from the surface.

600 Understanding the processes behind the measured fluxes is greatly helped by  
601 considering changes in the TAN budget of the surface (Supplementary Materials  
602 Section 5) and the accumulation of TAN varied greatly between sites. The most  
603 extreme variation was found for the simulated TAN budget at Ascension Island,  
604 where rapid NH<sub>3</sub> emission was reflected in almost complete loss of available TAN  
605 every evening. Under these circumstances, NH<sub>3</sub> emission is primarily controlled by  
606 the uric acid hydrolysis rate, as almost all the TAN produced (unless washed-off in  
607 rain) is immediately volatilized (Figure 2; Supplementary Material Section 2 Figure  
608 SM 2.1). A contrasting situation was found in the simulations for Bird Island and  
609 Signy Island, where TAN production (urea hydrolysis) is much slower than at the  
610 warm sites, average TAN Production is 0.10, 0.19 and 0.06 g m<sup>-2</sup> hr<sup>-1</sup> for Ascension  
611 Island, the Isle of May and Bird Island, respectively. Intermediate behaviour in the  
612 TAN budget was found at the Isle of May and Michaelmas Cay, with large diurnal  
613 variations, but still substantial night time values. At Michaelmas Cay, a large-scale  
614 structure in the TAN budget, varying over daily to weekly timescales was the effect of  
615 rain events on the available UA and TAN on the surface.

616

#### 617 **4.2 Process-based versus empirical approaches**

618 On a breeding season time-scale, temperature was shown to be the most influential  
619 meteorological variable, where NH<sub>3</sub> emission rate increases with increased  
620 temperature. Importantly this effect, which was identified empirically by Sutton et al.  
621 (2013) is here explained for the first time using a dynamic modelling approach  
622 comparing globally contrasting sites. This study therefore provides a substantial  
623 advance on initial empirical studies calculating NH<sub>3</sub> emissions from seabirds (Wilson  
624 et al. 2004; Blackall et al., 2007), which were used to calculate NH<sub>3</sub> emissions on a  
625 regional and country scale to Riddick et al. (2012).

626 The main limitation of the empirical approach of Riddick et al. (2012) was the wide  
627 uncertainty ranges related to the temperature effect and the need to constrain these by  
628 measurements, ideally using a process based approach. This is now addressed here.  
629 The GUANO model is able to explain the major differences between field sites, and  
630 the way that different variables contribute, including temperature, moisture  
631 availability and wind speed, as the most important drivers. A first application of the  
632 GUANO model reported by Sutton et al. (2013) to different sites globally showed that  
633 it was able to reproduce the main measured differences in the percentage of excreted  
634 guano that volatilizes as NH<sub>3</sub> in relation to temperature.

635 The major source of uncertainty is the value for pH used in the GUANO model. Even  
636 though the same value was used at the five colonies reported in this paper, the  
637 emission estimates calculated by the GUANO model was in good agreement with  
638 emission estimates based on concentration measurements and turbulent exchange  
639 parameters. This could suggest that the biogeochemical evolution of TAN from UA  
640 and subsequent formation of NH<sub>3</sub> happens independently of the substrate so that the  
641 pH of the underlying strata is less important. This is illustrated by the sensitivity  
642 analysis where a  $\pm 10\%$  alteration of substrate pH should equate to a sensitivity on  
643 instantaneous NH<sub>3</sub> emission potential of +605%, -86% (i.e. +/- factor of 7). The fact  
644 that the model outcome gave a net sensitivity on simulated NH<sub>3</sub> emissions for the Isle  
645 of May of only +73%, -22% illustrates that the amount of available TAN appears to  
646 constrain the total amount emitted and that more acid pH reduces urea hydrolysis rate  
647 (Equation SM5).

648

### 649 **4.3 NH<sub>3</sub> emissions globally**

650 The performance of the GUANO model is illustrated for the five colony emission  
651 estimates calculated by the GUANO model shown as the NH<sub>3</sub> emission normalized in  
652 relation to the seabird mass (Figure 6). The GUANO model emissions are in good  
653 agreement to emission estimates based on concentration measurements and turbulent  
654 exchange parameters when they are presented with matching emissions calculated  
655 from in-situ measurements by Riddick et al. (2014; 2016) and combined with  
656 measured emissions from other sites. The additional colonies represent rock nesters  
657 on the Isle of May (Blackall et al., 2007), a cold, dry Adélie penguin colony on  
658 Antarctica (Theobald et al., 2013) and a hot dry Double-crested cormorant colony on  
659 Mullet Island, California (Tratt et al., 2013). The consistency of the observed and  
660 model estimates shows that the GUANO model could be used to calculate NH<sub>3</sub>  
661 emissions from seabird colonies in a wide range of meteorological conditions. The  
662 GUANO model captures the large effect of NH<sub>3</sub> emission in response to temperature  
663 and can simulate the main differences between meteorology where emission rates per  
664 unit bird body mass vary across climates by more than an order of magnitude.

665 <<Insert Figure 6 Here>>

666 It is anticipated that NH<sub>3</sub> emissions from seabird colonies could change in a variety of  
667 ways when global climate change forecasts are considered. Changes to food supplies  
668 and changes in sea-level are both highlighted as drivers of future seabird population  
669 changes (Forcada et al., 2006; Trathan et al., 2007; Brierly, 2008). This, coupled with  
670 anticipated temperature increases in many parts of the Southern Ocean and the  
671 Antarctic Continent (Denvil, 2005), potentially present a very different N<sub>r</sub> landscape,  
672 associated with substantially increased NH<sub>3</sub> emissions. Through the GUANO model  
673 we now have a quantitative tool to assess such changes in N<sub>r</sub> partitioning which could  
674 be used to better forecast future changes to these remote nutrient-poor ecosystems.

### 675 **Acknowledgements**

676 The work described in this paper was supported by grants from the NERC CEH  
677 Integrating Fund and the NERC thematic programme (GANE). MAS and AM  
678 gratefully acknowledge support through the EU ÉCLAIRE project. We thank the  
679 Conservation Department on Ascension Island, Queensland Department of National  
680 Parks, Recreation, Sports and Racing, Scottish National Heritage, British Antarctic

681 Survey and Paul Hill of the University of Bangor for providing access/logistic  
682 support. We thank D. Briggs of BAS on Signy for information on meteorology and  
683 nesting penguins, and the BAS Bird Island crew for their technical and physical  
684 support (BAS CGS grant).

## 685 **References**

686 Adams, P. J., Seinfeld, J. H., Koch, D., Mickley, L., & Jacob, D. (2001) General  
687 circulation model assessment of direct radiative forcing by the sulfate-nitrate-  
688 ammonium-water inorganic aerosol system, *Journal of Geophysical Research-  
689 Atmospheres*, 106(D1), 1097-1111, doi:10.1029/2000JD900512.

690 Blackall, T.D. (2004) The emissions of ammonia from seabird colonies. PhD thesis,  
691 University of Leeds.

692 Blackall, T.D., Theobald, M.R., Milford, C., Hargreaves, K.J., Nemitz, E., Wilson,  
693 L.J., Bull, J., Bacon, P.J., Hamer, K.C., Wanless, S. and Sutton, M.A. (2004)  
694 Application of tracer ratio and inverse dispersion methods with boat-based plume  
695 measurements to estimate ammonia emissions from seabird colonies. *Water, Air, &  
696 Soil Pollution: Focus*, 4, 279-285.

697 Blackall, T. D., Wilson, L. J., Theobald, M. R., Milford, C., Nemitz, E., Bull, J.,  
698 Bacon, P. J., Hamer, K. C., Wanless, S. & Sutton, M. A. (2007) Ammonia emissions  
699 from seabird colonies. *Geophysical Research Letters*, 34, 5, 5-17.

700 Bogaard, A., Fraser, R.A., Heaton, T.H.E., Wallace, M., Vaiglova, P., Charles, M.,  
701 Jones, G., Evershed, R.P., Styring, A.K., Andersen, N.H., Arbogast, R.-M.,  
702 Bartosiewicz, L., Gardeisen, A., Kanstrup, M., Maier, U., Marinova, E., Ninov, L.,  
703 Schäfer, M. & Stephan, E., (2013) Crop manuring and intensive land management by  
704 Europe's first farmers, *Proceedings of the National Academy of Sciences* 110 (31),  
705 12589-12594.

706 Bouwman, A. F., Boumans, L. J. M. & Batjes, N. H. (2002) Estimation of global NH<sub>3</sub>  
707 volatilization loss from synthetic fertilizers and animal manure applied to arable lands  
708 and grasslands, *Global Biogeochemical Cycles*, 16(2), 1024,  
709 doi:10.1029/2000GB001389.

710 Brierley, A. S. (2008) Antarctic Ecosystem: Are deep krill ecological outliers or  
711 portents of a paradigm shift? *Current Biology*, 18, 252-254.

712 Cooter, E. J., Bash, J. O., Walker, J. T., Jones, M. R. & Robarge, W. (2010)  
713 Estimation of NH<sub>3</sub> bi-directional flux from managed agricultural soils, *Atmospheric  
714 Environment*, 44(17), 2107-2115, doi:10.1016/j.atmosenv.2010.02.044

715 Crittenden, P.D., Scrimgeour, C.S., Minnullina, G., Sutton, M.A., Tang, Y.S. &  
716 Theobald, M.R. (2015) Lichen response to ammonia deposition defines the footprint  
717 of a penguin rookery. *Biogeochemistry*. 122(2), 295-311.

718 Denvil, S. (2005) Intergovernmental Panel on Climate Change - Data Distribution  
719 Center. Accessed January 2016. URL was correct at a given date. [http://www.ipcc-  
720 data.org/](http://www.ipcc-data.org/).

721 Demmers, T.G.M., Burgess, L.R., Short, J.L., Phillips, V.R., Clark, J.A., & Wathes,  
722 C.M. (1998) First experiences with methods to measure ammonia emissions from  
723 naturally ventilated cow buildings in the UK. *Atmospheric Environment*, 32 (3), 285-  
724 293.

- 725 Elliott, H. A. & Collins, N. E. (1982) Factors affecting ammonia release in broiler  
726 houses. *Transactions of the ASAE*, 25, 413.
- 727 Elzing, A. & Monteny, G. J. (1997) Ammonia Emissions in a Scale Model of a Dairy-  
728 cow House. *Transactions of the ASAE*, 40, 713-720.
- 729 Flechard, C.R., Massad, R.-S., Loubet, B., Personne, E., Simpson, D., Bash, J.O.,  
730 Cooter, E.J., Nemitz, E. & Sutton, M.A. (2013) Advances in understanding, models  
731 and parameterisations of biosphere-atmosphere ammonia exchange. *Biogeosciences*  
732 10, 5385-5497.
- 733 Flesch, T.K., Wilson, J.D. and Yee, E. (1995) Backward-time Lagrangian stochastic  
734 dispersion models, and their application to estimate gaseous emissions. *Journal of*  
735 *Applied Meteorology*, 34, 1320-1332.
- 736 Forcada, J., Trathan, P. N., Reid, K., Murphy, E. J. and Croxall, J. P. (2006)  
737 Contrasting population changes in sympatric penguin species in association with  
738 climate warming. *Global Change Biology*, 12, 411-423.
- 739 Groot Koerkamp, P. W. G., Metz, J. H. M., Uenk, G. H., Phillips, V. R., Holden, M.  
740 R., Sneath, R. W., Short, J., L., White, R. P., Hartung, J., Seedorf, J., Schroder, M.,  
741 Linkert, K. H., Pedersen, S., Takai, H., Johnsen, J. O. & Wathes, C. M. (1998)  
742 Concentrations and emissions of ammonia in livestock buildings in Northern Europe.  
743 *Journal of Agricultural Engineering Research*, 70, 79-95.
- 744 Groot Koerkamp, P. W. G. (1994) Review on Emissions of Ammonia from Housing  
745 Systems for Laying Hens in Relation to Sources, Processes, Building Design and  
746 Manure Handling. *Journal of Agricultural Engineering Research* 59(2):73-87.
- 747 Harris, M.P. & Wanless, S. (2011) *The Puffin*. T. & A.D. Poyser, London. pp. 256.
- 748 Massad R.-S., Nemitz E. & Sutton M.A. (2010) Review and parameterisation of bi-  
749 directional ammonia exchange between vegetation and the atmosphere *Atmospheric*  
750 *Chemistry and Physics* 10, 10359-10386.
- 751 Nemitz, E., Sutton, M. A., Schjoerring, J. K., Husted, S. & Wyers, G. P. (2000)  
752 Resistance modelling of ammonia exchange over oilseed rape. *Agricultural and Forest*  
753 *Meteorology*, 105, 405-425.
- 754 Nemitz, E., Milford, C. & Sutton, M. A. (2001) A two-layer canopy compensation  
755 point model for describing bi-directional biosphere-atmosphere exchange of  
756 ammonia. *Quarterly Journal of the Royal Meteorological Society*, 127, 815-833.
- 757 Potter, P., Ramankutty, N., Bennett, E. M. & Donner, S. D. (2010), Characterizing  
758 the Spatial Patterns of Global Fertilizer Application and Manure Production, *Earth*  
759 *Interactions*, 14, 2, doi:10.1175/2009EI288.1.
- 760 Riddick, S. N., Dragosits, U., Blackall, T.D., Daunt, F., Wanless, S. & Sutton, M. A.  
761 (2012) The global distribution of ammonia emissions from seabird colonies,  
762 *Atmospheric Environment*, 55, 319-327, doi:10.1016/j.atmosenv.2012.02.052.
- 763 Riddick, S. N., Dragosits, U., Blackall, T.D., Daunt, F., Braban, C. F., Tang, Y. S.,  
764 MacFarlane, W., Taylor, S., Wanless S. & Sutton M. A. (2014) Measurement of  
765 ammonia emissions from tropical seabird colonies. *Atmospheric Environment*, 89, 35-  
766 42. 10.1016/j.atmosenv.2014.02.012.

- 767 Riddick, S. N., Dragosits, U., Blackall, T.D., Daunt, F., Braban, C. F., Tang, Y. S.,  
768 Newell, M., Schmale, J., Hill, P. W. Wanless S. & Sutton M. A. (2016) Measurement  
769 of ammonia emissions from temperate and polar seabird colonies. *Atmospheric*  
770 *Environment*. doi:10.1016/j.atmosenv.2016.03.016
- 771 Seinfeld, J. H. and Pandis, S. N. (2006) *Atmospheric Chemistry and Physics: From*  
772 *Air Pollution to Climate Change* London, John Wiley & Sons.
- 773 Sommer, S.G. & Christensen, B.T. (1991) Effect of dry matter content on ammonia  
774 loss from surface applied cattle slurry. In: Neilsen, V.C., Voorburg, J.H., L'Hermite,  
775 P. (Eds.), *Odour and Ammonia Emissions from Livestock Farming*. Elsevier, London,  
776 UK. pp. 141-147
- 777 Sommer, S. G. & Olesen, J. E. (2000) Modelling ammonia volatilization from animal  
778 slurry applied with trail hoses to cereals. *Atmospheric Environment*, 34, 2361-2372.
- 779 Sutton M.A., Asman W.A.H., Ellerman T., van Jaarsveld J.A., Acker K., Aneja V.,  
780 Duyzer J.H., Horvath L., Paramonov S., Mitosinkova M., Tang Y.S., Achermann B.,  
781 Gauger T., Bartnicki J., Neftel A. and Erisman J.W. (2003). Establishing the link  
782 between ammonia emission control and measurements of reduced nitrogen  
783 concentrations and deposition. *Environmental Monitoring and Assessment* **82** (2) 149-  
784 185.
- 785 Sutton, M. A., Fowler, D. & Moncrieff, J. B. (1993) The exchange of atmospheric  
786 ammonia with vegetated surfaces. 1. Unfertilized vegetation. *Quarterly Journal of the*  
787 *Royal Meteorological Society*, 119, 1023-1045.
- 788 Sutton M.A., Burkhardt J.K., Guerin D., Nemitz E. and Fowler D. (1998)  
789 Development of resistance models to describe measurements of bi-directional  
790 ammonia surface atmosphere exchange. *Atmospheric Environment* **32** (3), 473-480.
- 791 Sutton, M. A., Reis, S., Billen, G., Cellier, P., Erisman, J. W., Mosier, A. R., Nemitz,  
792 E., Sprent, J., van Grinsven, H., Voss, M., Beier, C. & Skiba, U. (2012), "Nitrogen &  
793 Global Change" Preface, *Biogeosciences*, 9(5), 1691-1693, doi:10.5194/bg-9-1691-  
794 2012.
- 795 Sutton, M.A., Reis, S., Riddick, S. N., Dragosits, U., Nemitz, E., Theobald, M.R.,  
796 Tang, Y.S., Braban, C.F., Vieno, M., Dore, A.J., Mitchell, R.F., Wanless, S., Daunt,  
797 F., Fowler, D., Blackall, T.D., Milford, C., Flechard, C.R., Loubet, B., Massad, R.,  
798 Cellier, P., Personne, E., Coheur, P.F., Clarisse, L., Van Damme, M., Ngadi, Y.,  
799 Clerbaux, C., Skjoth, C.A., Geels, C., Hertel, O., Kruit, R.J.W., Pinder, R.W., Bash,  
800 J.O., Walker, J.T., Simpson, D., Horvath, L., Misselbrook, T.H., Bleeker, A.,  
801 Dentener, F. & de Vries, W. (2013) Towards a climate-dependent paradigm of  
802 ammonia emission and deposition. *Philosophical Transactions of the Royal Society*  
803 *B-Biological Sciences* 368, pp.20130166.
- 804 Tang, Y. S., Cape, J. N. & Sutton, M. A. (2001) Development and types of passive  
805 samplers for NH<sub>3</sub> and NO<sub>x</sub>. In *Proceedings of the International Symposium on*  
806 *Passive Sampling of Gaseous Pollutants in Ecological Research*. The Scientific  
807 *World*, 1, 513-529.
- 808 Theobald, M.R., Crittenden, P.D., Tang, Y.S. & Sutton, M.A. (2013) The application  
809 of inverse-dispersion and gradient methods to estimate ammonia emissions from a  
810 penguin colony. *Atmospheric Environment* 81:320–329.

- 811 Trathan, P. N., Forcada, J. and Murphy, E. J. (2007) Environmental forcing and  
812 Southern Ocean marine predator populations: effects of climate change and  
813 variability. *Philosophical Transactions of the Royal Society B-Biological Sciences*,  
814 362, 2351-2365.
- 815 Tratt, D, M., Buckland, K. N., Young, S. J., Johnson, P.D., Riesz K. A., & Molina K.  
816 C. (2013) Remote sensing visualization and quantification of ammonia emission from  
817 an inland seabird colony. *Journal of Applied Remote Sensing*. 7(1), pp. 073475.
- 818 Wentworth, G. R., Murphy, J. G., Croft, B., Martin, R. V., Pierce, J. R., Côté, J.-S.,  
819 Courchesne, I., Tremblay, J.-É., Gagnon, J., Thomas, J. L., Sharma, S., Toom-  
820 Saunry, D., Chivulescu, A., Levasseur, M., & Abbatt, J. P. D. (2015) Ammonia in the  
821 summertime Arctic marine boundary layer: sources, sinks and implications,  
822 *Atmospheric Chemistry Physics Discussions*, 15, 29973-30016, doi:10.5194/acpd-15-  
823 29973-2015.
- 824 Wilson, L. J., Bacon, P. J., Bull, J., Dragosits, U., Blackall, T. D., Dunn, T. E.,  
825 Hamer, K. C., Sutton, M. A. & Wanless, S. (2004) Modelling the spatial distribution  
826 of ammonia emissions from seabirds in the UK. *Environmental Pollution*, 131, 173-  
827 185.
- 828 Zhu, R.B., Sun, J.J., Liu, Y.S., Gong, Z.J., & Sun, L.G. (2011) Potential ammonia  
829 emissions from penguin guano, ornithogenic soils and seal colony soils in coastal  
830 Antarctica: effects of freezing-thawing cycles and selected environmental variables.  
831 *Antarctic Science* 23, 78-92.
- 832

833 Table 1 Data used in the GUANO model.  $D_{met}$  is the distance from meteorological  
834 stations to each colony.  $F_{hab}$  values describe the fraction  $NH_3$  that is captured by the  
835 substrate and overlying vegetation (Supplementary Material Section 1, Table SM1.1).  
836 Site-specific seabird data input to the GUANO model were collated from field  
837 observation (nest density and duration of breeding season ( $D$ )) and from the literature  
838 (adult mass, fraction of time at colony ( $FC$ ), see Riddick et al., 2012). The nitrogen  
839 excretion rate at colony ( $F_e$ ) is calculated using Equation 1 in this study.

840

841 Table 2 Comparison between the measured  $NH_3$  emissions and  $NH_3$  emissions  
842 simulated using the GUANO model for Michaelmas Cay, Great Barrier Reef,  
843 Australia during Period 1 (5/11/2009 to 10/12/2009) & Period 2 (10/12/2009 to  
844 6/1/2010) and Signy Island during Period 1 (10/01/09 - 25/01/09), Period 2 (25/01/09  
845 - 08/02/09) and Period 3 (08/02/09 - 21/02/09). Measured values from Riddick et al.  
846 (2014; 2016).

847

848 Table 3 Comparison between measured  $NH_3$  emissions and  $NH_3$  emission simulated  
849 using the GUANO model for the measurement periods at different study sites.  $P_v$  is  
850 the percentage of N volatilized as  $NH_3$ . Determination coefficients ( $R^2$ ) are shown for  
851 modelled emissions based on hourly data between modelled  $NH_3$  emission and each  
852 climate variable and for the comparison of modelled and measured emissions (value  
853 after each  $R^2$  in brackets shows + or - interaction). The mean modelled % of  
854 available TAN emitted was calculated from the total emission and the total duration  
855 of the measurement period. The climate variables  $T_g$  represents Ground Temperature,  
856  $RH$  is relative humidity,  $WS$  is wind speed and  $P$  is precipitation. For Michaelmas  
857 Cay and Signy Island, denoted by <sup>a</sup>, the values are a time-weighted mean of the  
858 measurement and model values shown in Table 2.

859

860 Table 4 Sensitivity analysis of total modelled  $NH_3$  emission for the Isle of May  
861 (28/06/10 to 23/07/10) using the GUANO model. C indicates a constant and V  
862 indicates a variable. For the meteorological variables, each hourly value used for  
863 ground temperature, relative humidity, wind speed, precipitation and net solar  
864 radiation is varied by  $\pm 10\%$ . <sup>+</sup> the average value for each meteorological variable  
865 from 28/06/10 to 23/07/10 is given. <sup>x</sup> denotes  $F_{hab}$  for the Isle of May, other  $F_{hab}$   
866 values are given in Table 1.1 in Supplementary Material Section 1.

867

868

869

870

871 Figure 1 Schematic of the GUANO model. Pathways taken by nitrogen following  
872 excretion as uric acid (after Blackall, 2004 modified). The numbers illustrate an  
873 example where the total mass of excreta (M) is made from 0.6 M of water, 0.21 M of  
874 uric acid and 0.19 M of non-N guano. TAN is Total Ammoniacal Nitrogen.

875

876 Figure 2 Comparison between measured and modelled  $\text{NH}_3$  emissions for the Sooty  
877 tern colony at Mars Bay, Ascension Island (22<sup>nd</sup> May to 10<sup>th</sup> June 2010). Top panel:  
878 Rain, ground temperature, relative humidity and wind speed (measured values).  
879 Middle panel: Guano water and TAN (modelled values). Bottom Panel: Measured  
880 and modelled  $\text{NH}_3$  emissions. The  $F_{hab}$  value used in the GUANO model was 0.67  
881 (based on a sand substrate). All values are hourly; tick marks on the x-axis indicate  
882 midnight.

883

884 Figure 3 Comparison between measured and modelled  $\text{NH}_3$  emissions for the Isle of  
885 May, Scotland (5<sup>th</sup> to 26<sup>th</sup> July, 2009). Top panel: Rain, ground temperature, relative  
886 humidity and wind speed (measured values). Middle panel: Guano water and TAN  
887 (modelled values). Bottom Panel: Measured and modelled  $\text{NH}_3$  emission. The  $F_{hab}$   
888 value used in the GUANO model was 0.64 (based on a soil/rock substrate). All  
889 values are hourly; tick marks on the x-axis indicate midnight.

890

891 Figure 4 Comparison of measured and modelled  $\text{NH}_3$  emissions from the Big Mac  
892 Macaroni penguin colony, Bird Island, South Georgia (18/11/2010 to 13/12/2010).  
893 Top panel: Rain, ground temperature, relative humidity and wind speed (measured  
894 values). Middle panel: Guano water and TAN (modelled values). Bottom panel:  
895 Measured and modelled  $\text{NH}_3$  emission. The  $F_{hab}$  value used in the GUANO model  
896 was 1 (based on a rock substrate). All values are hourly; tick marks on the x-axis  
897 indicate midnight.

898

899 Figure 5 Comparison between monthly time-integrated measured  $\text{NH}_3$  emission with  
900 modelled hourly  $\text{NH}_3$  emissions and monthly-mean modelled emissions for A.  
901 Michaelmas Cay, Great Barrier Reef, Australia (5/11/2009 to 1/1/2010) and B. Signy  
902 Island (10/01/09 to 21/02/09). Measured ground temperature ( $^{\circ}\text{C}$ ) and modelled TAN  
903 amount ( $\text{g m}^{-2}$ ) are shown for comparison. Tick marks on the x-axis indicate  
904 midnight. The  $F_{hab}$  values were 0.67 (sand) and 1 (rock) for Michaelmas Cay and  
905 Signy Island, respectively.

906

907 Figure 6 Measured amount of excreted  $\text{N}_r$  that is volatilized as  $\text{NH}_3$  as a function of  
908 mean temperature during different field campaigns as compared with estimates of the  
909 GUANO model. The line shows the best fit of the measured data ( $\text{NH}_3$  ( $\mu\text{g g (bird)}^{-1}$   
910  $\text{s}^{-1}$ ) =  $0.0014e^{0.1099T}$ ;  $R^2 = 0.96$ ). The field site codes are: C.H., Cape Hallett,  
911 Antarctica; S.I., Signy Island; B.I., Bird Island, South Georgia; I.M., Isle of May,  
912 Scotland, (b) – burrows, (c) - cliffs; B.R., Bass Rock, Scotland; M.C., Michaelmas  
913 Cay, Australia; A.I., Ascension Island; M.I., Mullet Island, California.

914

915

916

Colony	Target Species	Population (Pairs)	Measurement strategy	Av <i>T</i> (°C)	Av <i>RH</i> (%)	Av <i>WS</i> (m s <sup>-1</sup> )	<i>D</i> <sub>met</sub> (km)	<i>F</i> <sub>hab</sub>	Adult Mass (g)	Nest Density (m <sup>-2</sup> )	Breeding season <i>D</i> (days)	<i>FC</i>	N excretion rate <i>F</i> <sub>e</sub> (g m <sup>-2</sup> hr <sup>-1</sup> )	Average Measured NH <sub>3</sub> Emission (μg m <sup>-2</sup> s <sup>-1</sup> )
Ascension Island 7.99 °S, 14.39 °W	Sooty tern	100,000	Active	27	72	5	2	0.67	190	1.26	122	0.6	0.14	30.2 <sup>a</sup>
Isle of May 56.19 °N, 2.56 °W	Atlantic puffin	20,000	Active	15	80	4	1	0.60	410	1.27	152	0.3	0.13	5.0 <sup>b</sup>
Bird Island 54.01 °S, 38.08 °W	Macaroni penguin	40,000	Active	3	92	5	5	1.00	4680	0.85	213	0.6	1.13	12.9 <sup>b</sup>
Michaelmas Cay 16.60°S, 145.97°E	Common noddy	12,000	Passive	28	85	5	17	0.67	200	1.70	122	0.6	0.20	22.3 <sup>a</sup>
Signy Island 60.73° S, 45.58° W	Adélie and Chinstrap penguin	19,000	Passive	2	84	5	50	1.00	4150	0.63	274	0.6	0.79	9.0 <sup>b</sup>

<sup>a</sup>Riddick et al. (2014)

<sup>b</sup>Riddick et al. (2016)

ACCEPTED MANUSCRIPT

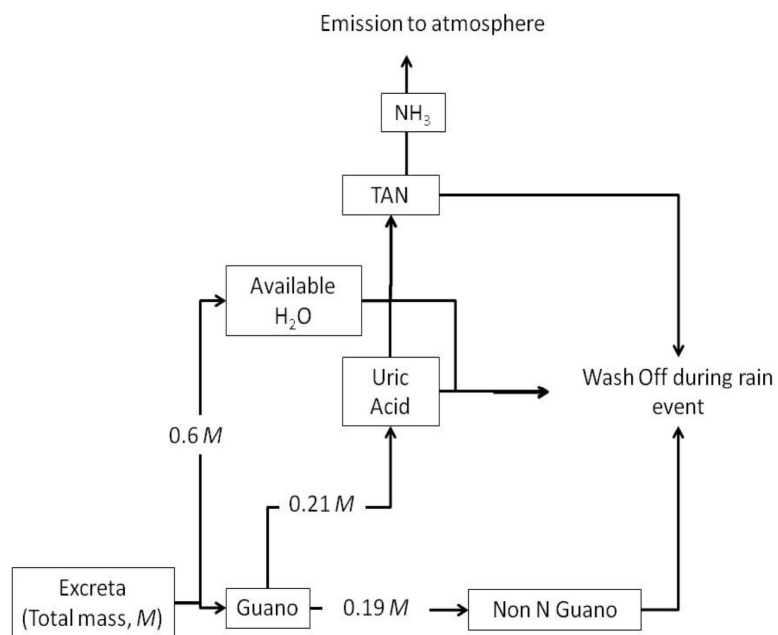
	Michaelmas Period 1	Michaelmas Period 2	Signy Period 1	Signy Period 2	Signy Period 3
Measured emission ( $\mu\text{g NH}_3 \text{ m}^{-2} \text{ s}^{-1}$ )	21.3	22.2	18.2	7.9	9.0
GUANO Model emission ( $\mu\text{g}$ $\text{NH}_3 \text{ m}^{-2} \text{ s}^{-1}$ )	25.1	29.9	16.7	9.7	10.7
Difference between measured and modelled (%)	15.0	25.8	-8.3	22.9	18.4

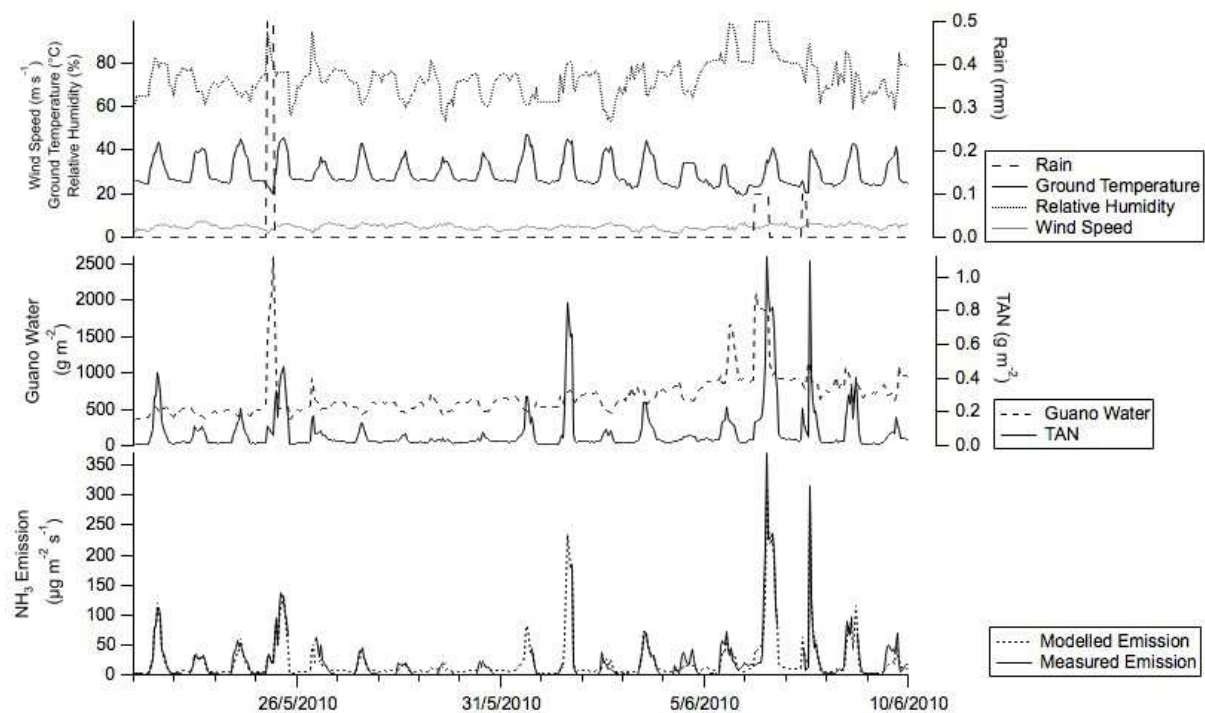
Colony	NH <sub>3</sub> emission ( $\mu\text{g m}^{-2} \text{s}^{-1}$ )		$P_v$ (%)		$R^2$ between hourly modelled NH <sub>3</sub> emission and meteorological variable				Comparison of hourly modelled to hourly measured emissions			
	Measured	GUANO Model	Measured	GUANO Model	$T_g$	$RH$	$WS$	$P$	$R^2$	Slope	Intercept ( $\mu\text{g m}^{-2} \text{s}^{-1}$ )	Modelled mean % of available TAN emitted as NH <sub>3</sub> in a day <sup>x</sup>
Ascension Island	30.2	21.5	51.9	37.0	0.11 (+)	0.01 (+)	0.01 (+)	0.03 (+)	0.94	1.07	-1.2	67.0
Isle of May	5.0	3.2	4.7	2.8	0.39 (+)	0.04 (-)	0.06 (+)	0.01 (+)	0.13	0.13	5.7	5.5
Bird Island	12.9	12.7	1.8	1.7	0.39 (+)	0.04 (-)	0.59 (+)	0.01 (+)	0.86	1.09	-1.3	1.6
Michaelmas Cay <sup>a</sup>	22.3	27.5	66.8	82.4	0.18 (+)	0.04 (-)	0.01 (+)	0.01 (-)				20.9
Signy Island <sup>a</sup>	9.0	10.7	2.4	2.9	0.38 (+)	0.03 (-)	0.22 (+)	0.01 (+)				0.11

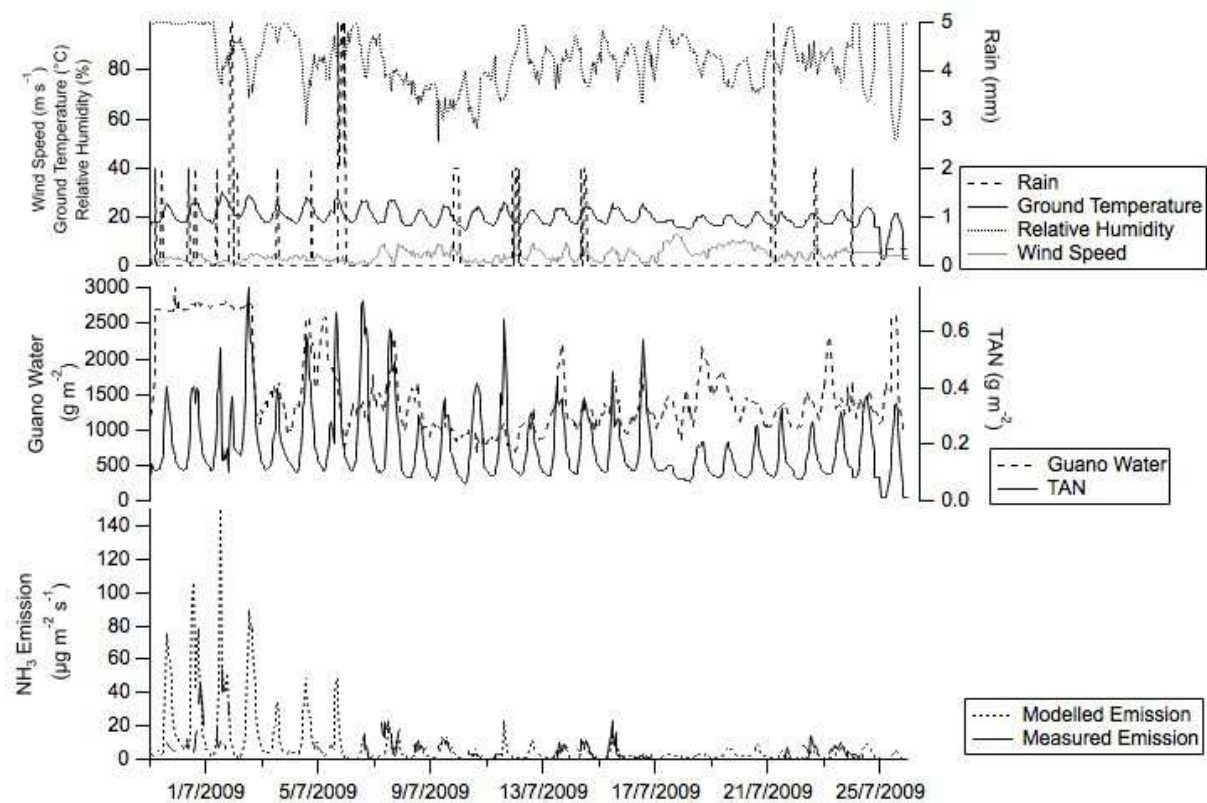
<sup>x</sup>, this is defined as the average percentage of TAN produced in a day that volatilizes as NH<sub>3</sub>

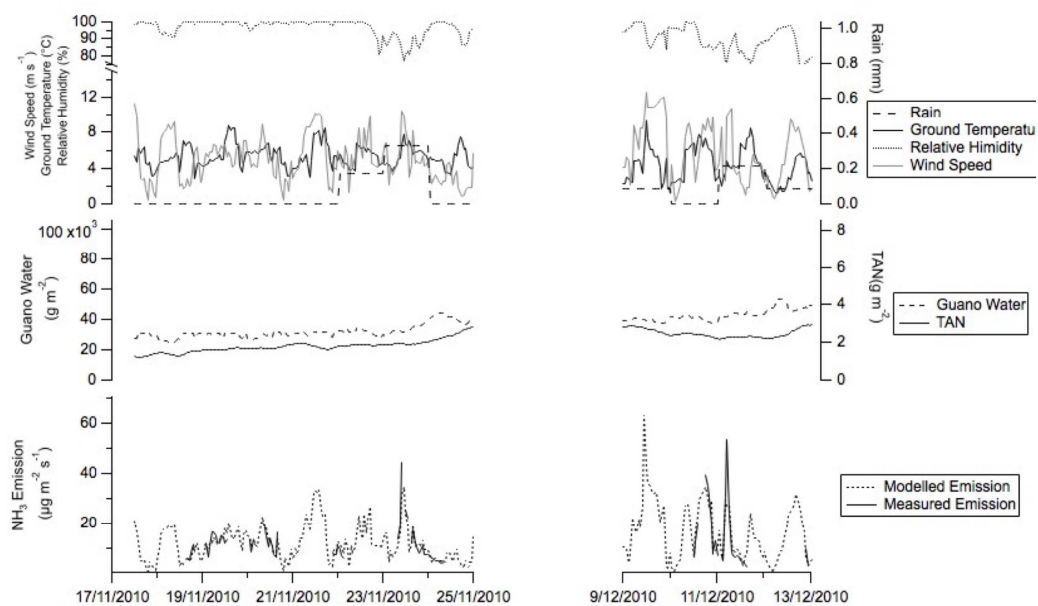
ACCEPTED MANUSCRIPT

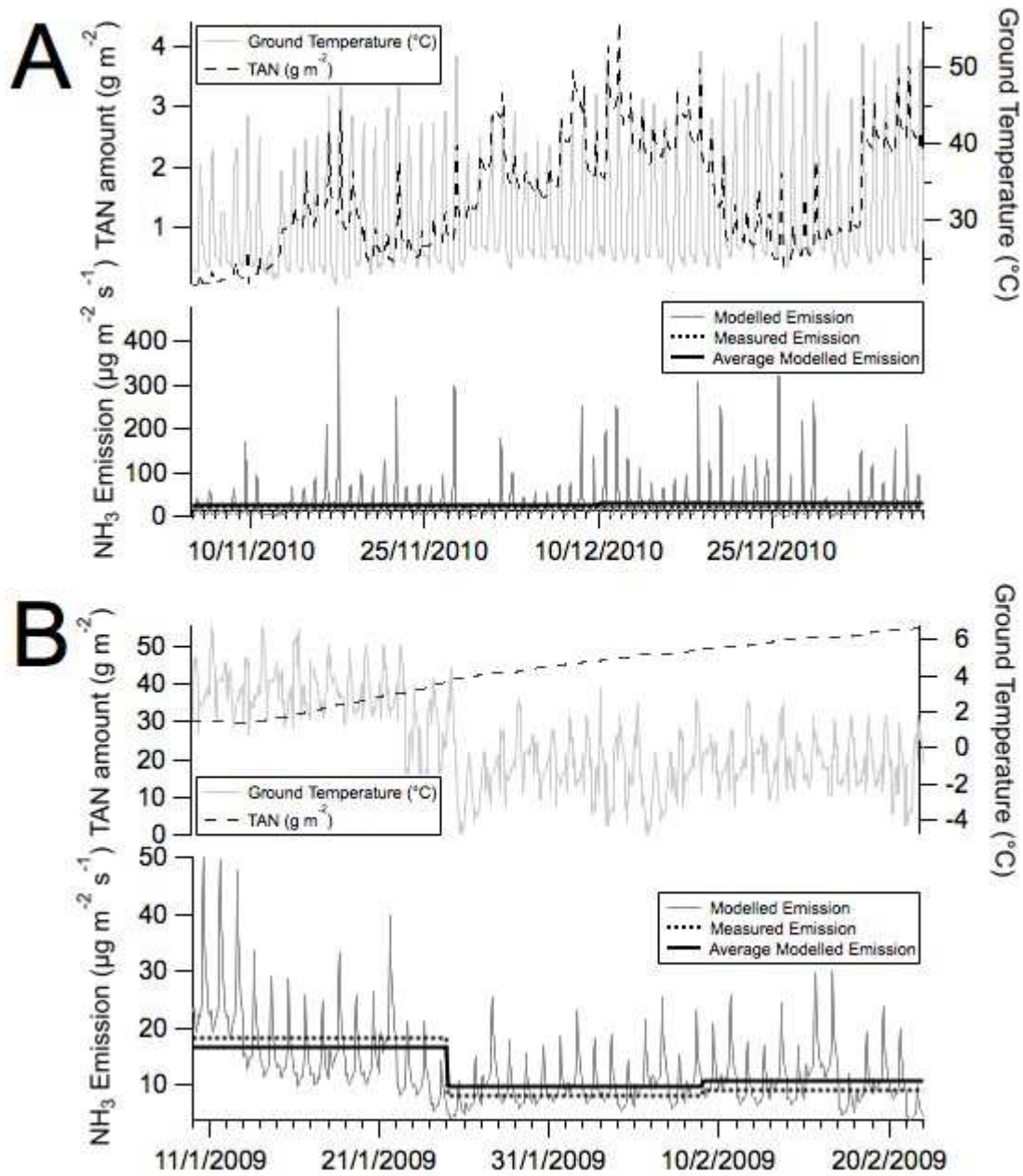
Factor	Type	Base value for all model runs (and range tested)		Source of base value	% Change in NH <sub>3</sub> emission	
					High Value	Low Value
Surface roughness height ( $z_0$ , m)	C	0.1	(0.01 – 0.5)	Seinfeld and Pandis (2006) Riddick et al. (2014; 2016)	+70	-56
UA conversion to TAN (% day <sup>-1</sup> at pH 9, T = 35 °C)	C	0.83	(±10%)	Elliot and Collins (1982)	-9.42	9.30
Nitrogen wash off (% mm <sup>-1</sup> rain)	C	1	(±10%)	Blackall (2004)	8.19	-7.12
Non-Nitrogen Wash off (% mm <sup>-1</sup> rain)	C	0.5	(±10%)	Blackall (2004)	-0.15	+0.17
Boundary layer Stanton number ( $B$ )	C	5	(±10%)	Sutton et al. (1993)	+0.04	-0.04
Habitat Factor ( $F_{hab}$ ) <sup>x</sup>	C	0.60	(0.2 – 1)	Wilson et al. (2004) Riddick (2012)	-70	+49
Substrate pH	C	8.5	(7 – 9)	Blackall (2004)	+73	-22
Background NH <sub>3</sub> concentration (µg m <sup>-3</sup> )	C	0.1	(±10%)	Sutton et al. (2003)	-0.02	+0.01
Ground Temperature ( $T$ , °C)	V	20 <sup>+</sup>	(±10%)	Measured	-36.8	+59.9
Relative Humidity ( $RH$ , %)	V	84 <sup>+</sup>	(±10%)	Measured	-13.0	+6.7
Wind Speed ( $U$ , m s <sup>-1</sup> )	V	4.3 <sup>+</sup>	(±10%)	Measured	-11.0	+12.9
Precipitation ( $P$ , mm m <sup>-2</sup> hr <sup>-1</sup> )	V	0.17 <sup>+</sup>	(±10%)	Measured	+20.7	-11.8
Net solar radiation ( $R_n$ , Wm <sup>-2</sup> )	V	82.6 <sup>+</sup>	(±10%)	Measured	-2.1	+1.2



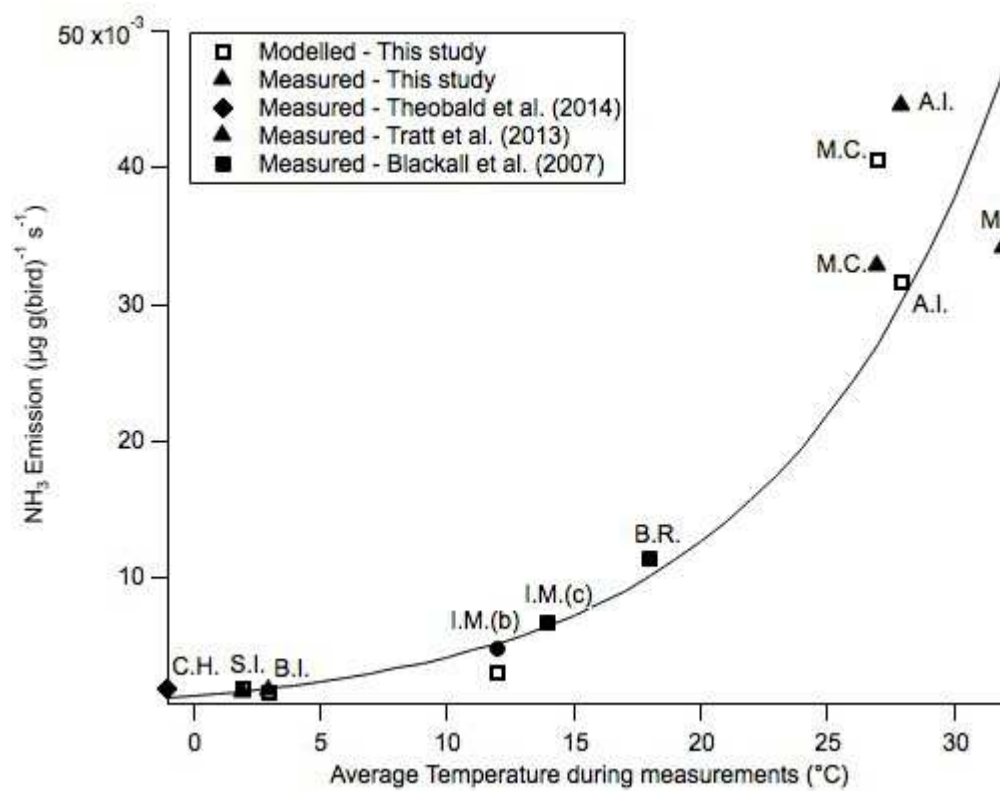








ACC



- > A dynamic mass-flow model to simulate variation in  $\text{NH}_3$  emissions from seabird guano
- > Model output validated against measurements from colonies across a range of climates
- > Model output captures observed dependence of  $\text{NH}_3$  emission on environmental variables
- > This model can be a starting point to model  $\text{NH}_3$  emissions from other sources

ACCEPTED MANUSCRIPT